



# Capillary electrophoresis–inductively coupled plasma–mass spectrometry hyphenation for the determination at the nanogram scale of metal affinities and binding constants of phosphorylated ligands

Fanny Varenne<sup>a</sup>, Mélanie Bourdillon<sup>b</sup>, Michel Meyer<sup>b,\*</sup>, Yi Lin<sup>c</sup>, Marie Brellier<sup>d</sup>, Rachid Baati<sup>d</sup>, Loïc J. Charbonnière<sup>a</sup>, Alain Wagner<sup>d</sup>, Eric Doris<sup>c</sup>, Frédéric Taran<sup>c</sup>, Agnès Hagée<sup>e,f,\*\*</sup>

<sup>a</sup> UMR CNRS 7178 IPHC-DSA, ECPM, Laboratoire d'Ingénierie Moléculaire Appliquée à l'Analyse, ECPM Bât R1N0, 25 rue Becquerel, 67087 Strasbourg, France

<sup>b</sup> Institut de Chimie Moléculaire de l'Université de Bourgogne (ICMUB), UMR CNRS 5260, 9 Avenue A. Savary, 21078 Dijon Cedex, France

<sup>c</sup> CEA, Service de Chimie Bioorganique et de Marquage, iBiTecS, 91191 Gif sur Yvette, France

<sup>d</sup> Université de Strasbourg, Faculté de Pharmacie, Laboratory of Functional ChemoSystems, UMR CNRS 7199, 67401 Illkirch–Graffenstaden, France

<sup>e</sup> CNRS UMR 6191, CEA Cadarache, DSV iBEB, 13108 St. Paul Les Durance, France

<sup>f</sup> CEA Marcoule, DSV iBEB, Service de Biochimie et de Toxicologie Nucléaire, 30207 Bagnols sur Cèze, France

## ARTICLE INFO

### Article history:

Received 29 November 2011

Received in revised form 20 January 2012

Accepted 23 January 2012

Available online 31 January 2012

### Keywords:

Speciation

Solution equilibrium studies

Binding constants

Microchemistry

Lanthanide

Europium

## ABSTRACT

A screening strategy based on hyphenated capillary electrophoresis and inductively coupled plasma mass spectrometry (CE–ICP–MS) was developed to classify phosphorylated ligands according to their europium(III) binding affinity in a hydro-organic medium (sodium formate, pH 3.7, H<sub>2</sub>O/MeOH 90:10, v/v). Taking advantage of the high sensibility of ICP–MS for detecting phosphorus, this method enabled to assess the affinity of a variety of phosphorylated compounds, including phosphine oxides, thiophosphines, phosphonates, and phosphinates, in less than 1 h and using less than 5 ng of substance. By varying the total europium concentration, complexation constants could be determined according to a sequential multiple run strategy, which proved to be in excellent agreement with the values obtained by UV–Vis absorption spectrophotometric titrations.

© 2012 Elsevier B.V. All rights reserved.

## 1. Introduction

Combinatorial synthesis experiences an ever-growing success in the discovery of new functional targets, such as drugs or catalysts [1]. The different synthetic routes adopted (mainly divergent and parallel synthesis) lead to a wide range of new compounds, which have to be selected regarding their intrinsic properties. Therefore, the success of such strategies requires the concomitant development of fast and sensitive screening tools [2]. Numerous efforts have been undertaken, especially in the field of catalysis, to propose new analytical means able to evaluate catalytic activities. Based on the benefits in terms of cost and speed, these new synthetic approaches have been extended to other fields. As an efficient alternative to the classical route of rational ligand design that rests on

the molecular engineering principles [3], Dam et al. exploited for the first time in 2008 the concepts of combinatorial chemistry for preparing receptors possessing a higher affinity for actinides over lanthanides [4,5].

Our own research in the field of parallel synthesis has afforded several large chemical libraries of phosphorus-containing multi-dentate ligands aimed at the selective complexation of lanthanides and actinides [6,7]. Considering the large number of synthesized molecules, which were often only available at the milligram scale, the development of a fast and reliable screening tool able to evaluate the potential of these compounds in terms of metal ion binding affinity became mandatory. A first step towards this goal was achieved recently when some of us disclosed a simple and fast colorimetric displacement assay allowing to rank the ligands according to their affinity towards uranium(VI) [6]. Carried out in microwell plates, the test allowed to classify the conditional binding constant ( $K_{\text{cond}}$ ) into 5 categories according to the absorbance changes of sulfochlorophenol S induced at a given pH by competitive UO<sub>2</sub><sup>2+</sup> uptakes by both the analyzed and chromogenic chelators. Following this approach,  $K_{\text{cond}}$  values could be bracketed at best within 0.4 logarithmic units. A more precise

\* Corresponding author. Tel.: +33 3 80 39 37 16; fax: +33 3 80 39 61 17.

\*\* Corresponding author at: CNRS UMR 6191, CEA Cadarache, DSV iBEB, 13108 St. Paul Les Durance, France. Tel.: +33 4 66 79 19 88; fax: +33 4 66 79 19 05.

E-mail addresses: [michel.meyer@u-bourgogne.fr](mailto:michel.meyer@u-bourgogne.fr) (M. Meyer), [agnes.hagege@cea.fr](mailto:agnes.hagege@cea.fr) (A. Hagée).

quantitative assessment of the metal-ligand equilibrium constants can be classically achieved by monitoring the changes of some physico-chemical properties of the system during a titration experiment. Potentiometry and spectrophotometry are among the most useful and widespread techniques, albeit they are rather time-consuming and not adapted to the study of either highly dilute solutions (glass-electrode potentiometry requires millimolar or higher concentration levels), ligands possessing no protonation sites, or UV-Vis transparent chemicals. Although more sensitive, laser-induced fluorescence spectroscopy [8–12] is restricted to systems involving fluorophore-bearing organic ligands and/or luminescent cations, as for example  $\text{Eu}^{3+}$ ,  $\text{Tb}^{3+}$ ,  $\text{Am}^{3+}$ , or  $\text{Cm}^{3+}$  [11,13–15], and thus cannot be considered as a general purpose analytical tool.

In that context, capillary electrophoresis appears extremely appealing, owing to the commercial availability of fully automated instrumentation and the consumption of very small sample volumes not exceeding a few  $\mu\text{L}$ . Moreover, affinity capillary electrophoresis (ACE) has become a mature separation technique that has been successfully applied for the measurement of stability constants of many chemical, biochemical, and biological systems [16–18], including protonation constants of weak bases [19,20], association constants of metal/ligand [21–24], metal/biomolecule [25–28], or drug/protein complexes [29–31], provided that the formation and dissociation kinetics are fast (formation of labile species). However, common systems equipped with UV detectors do not usually possess the required sensitivity for analyzing minute amounts of ligands. To overcome these limitations, hyphenation between capillary electrophoresis and plasma ionization mass spectrometry has emerged as a highly efficient speciation tool for solution equilibrium studies, considering the very low detection limits of ICP-MS instruments which are typically in the part per trillion (ppt) or nanogram per liter range.

Taking advantage of this particular feature, 1:1 complexes stability constants [22] but also successive 1:1 and 1:2 metal-ligand constants [23] were reported in the case of uranyl and lanthanum-oxalate complexes using up to 0.1 M oxalate in the electrolyte. Attempts to reduce ligand amounts were also reported for complexes presenting lower exchange kinetics by direct injection of metal solutions incubated with proteins [32,33] or phytosiderophores [34]. However, only conclusions about relative binding constants can be drawn.

We devised here a rapid screening methodology based on the mass-spectral monitoring of the  $\text{P}^+$  signal, which enables in a single analytical run to classify a library of ligands according to their increasing metal-binding affinity. Moreover, sequential multiple run experiments enabled to accurately estimate metal/ligand association constants, even in the case of multiple overlapping equilibria. As a proof of principle, this approach has been exemplified hereafter on a series of phosphorus-containing europium(III) chelators (Fig. 1) that were obtained on milligrams scale by combinatorial chemistry.

## 2. Materials and methods

### 2.1. Chemicals and solutions

All reagents were of analytical grade and were used without further purification. For the separation buffers, increasing amounts of  $\text{EuCl}_3 \cdot 6\text{H}_2\text{O}$  (Aldrich) were dissolved in a 25 mM formic acid (Pro-labo) solution, adjusted to pH 3.7 with 1 M NaOH, and prepared in a water/methanol 90:10 (v/v) mixture. The chloride concentration was maintained constant at 30 mM by addition of NaCl (Carlo Erba). A 5 mM formic acid aqueous solution containing 2  $\mu\text{g/L}$  of  $\text{In}^{3+}$  was used as make-up solution. Both separation buffer and make-up

**Table 1**  
ICP-MS operating conditions.

MS detector	Quadrupole equipped with a collision cell
Radiofrequency power	1550 W
Coolant gas flow	15 L $\text{min}^{-1}$
Auxiliary gas flow	0.8 L $\text{min}^{-1}$
Nebulizer gas flow	1 L $\text{min}^{-1}$
Spray chamber temperature	2 °C
Integration time	3.0 s for $^{31}\text{P}$ , 0.3 s for $^{115}\text{In}$

solution were freshly prepared on a daily basis and filtered through a 0.45  $\mu\text{m}$  membrane (Analytapore). Methanol (Carlo Erba) and NaOH (SDS) were used for the capillary conditioning. Phosphorylated ligands 1–15 (Fig. 1), synthesized according to previously described procedures [7], were dissolved in water/methanol mixtures (90:10, v/v) at a concentration of ca. 0.1 mM.

### 2.2. Capillary electrophoresis

Experiments were carried out on a Beckman P/ACE MDQ capillary electrophoresis instrument (CE) controlled by the 32 Karat software. The untreated fused-silica capillaries (80 cm  $\times$  75  $\mu\text{m}$  inner diameter, 375  $\mu\text{m}$  outer diameter) were purchased from Composite Metal Services Ltd. Before the first use, the capillary was washed at 138 kPa with methanol for 3 min, followed by ultra-pure water for 5 min, and 1 M NaOH for 3 min. The inner surface was then dynamically coated with polybrene for 25 min. For that purpose, a 0.5% m/m polybrene (Aldrich) solution was prepared in ultra-pure water to which a large excess of AG MP-1 anion exchange resin in its chloride form (Bio-Rad, capacity: 1.0 mequiv./mL) was added. The exchange was carried out for 2 h. After filtration, this solution was diluted to 0.1% (m/m) in the formic acid/sodium chloride separation buffer and used for capillary inner surface modification. Between successive runs, the capillary was flushed at 138 kPa with the running buffer containing 0.1% (m/m) polybrene for 10 min, then with the running buffer for 3 min.

The ICP-MS instrument used as detector was a 7500 ce model from Agilent Technologies. The spectrometer was controlled by the MassHunter software and was equipped with a MicroMist nebulizer (0.1 mL/min, Glass Expansion). The optimized operating conditions are summarized in Table 1. Hyphenation was achieved via a home-made sheath-flow interface described elsewhere [32], used to introduce the CE eluent into the MicroMist nebulizer. The capillary goes first through a microcross piece toward the tip of the nebulizer, 1 mm from the beginning of the inner solution capillary. The sheath-flow solution was introduced by self-aspiration through the third inlet of the microcross piece. The electrical connection was achieved by the ground electrode positioned through the fourth inlet of the microcross. The make-up solution flask was positioned on an elevator so that its height could be adjusted to eliminate the suction effect due to the nebulizer using the following procedure: the background noise was first monitored by ICP-MS at  $m/z = 115$ . The capillary was then completely filled with an indium nitrate solution (4.6 mg/L  $\text{In}^{3+}$ ) and the  $^{115}\text{In}$  signal was recorded. The height of the make-up solution was gradually increased until the signal reached the initial background noise level. Finally, the capillary was filled with the buffer solution and a 15 kV voltage was applied. By monitoring the current, it was ensured that the make-up solution was not driven back in the capillary, as this would result in a decrease of the current.

Separations were performed using a series of formate buffers with increasing concentrations of europium chloride (from 0 to 10 mM). The total chloride concentration was kept constant at 30 mM by adding appropriate amounts of NaCl. The electroosmotic mobility ( $\mu_{\text{eo}}$ ) was measured at 200 nm and deduced from the migration time of the water contained in the samples. The latter

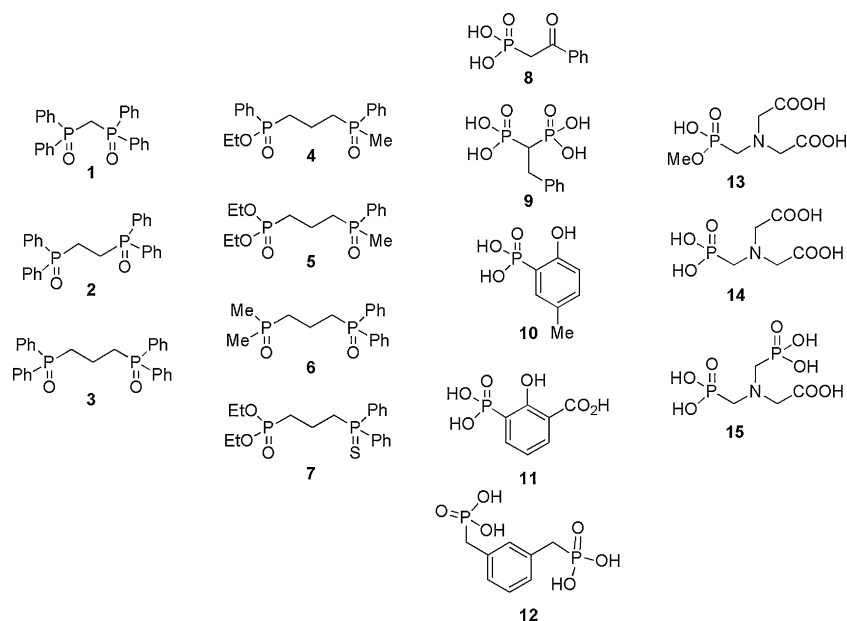


Fig. 1. Phosphorylated compounds examined in this study.

were injected for 5 s at 3.45 kPa, corresponding to ca. 25 nL. Separations were carried out at  $-20$  kV and  $25^\circ\text{C}$ .

In capillary electrophoresis, the apparent mobility of ionic species,  $\mu_{\text{app}}^{\text{L}}$ , can be determined using the following equation:

$$\mu_{\text{app}}^{\text{L}} = \frac{L_{\text{det}}L}{tV} \quad (1)$$

where  $L_{\text{det}}$  is the length from the capillary inlet to the detector,  $L$  is the capillary full length,  $t$  is the migration time and  $V$ , the applied voltage.

Since  $\mu_{\text{app}}^{\text{L}}$  is a combination of both the effective electrophoretic and the electroosmotic mobilities,  $\mu_{\text{ep}}^{\text{L}}$  in the different electrolytes can be deduced from Eq. (2):

$$\mu_{\text{ep}}^{\text{L}} = \mu_{\text{app}}^{\text{L}} - \mu_{\text{eo}} \quad (2)$$

Since all experiments were performed in triplicate, the reported electrophoretic mobilities correspond to the arithmetic mean values and their uncertainties to the associated standard deviation. These data were further processed by unweighed nonlinear least-squares using the Origin 6.0 software [35]. The choice of a constant weighing scheme ( $\omega_i = 1$ ) was fully justified by the nearly constant errors found for the mobilities over the entire europium concentration range.

### 2.3. Spectrophotometric titrations

All solutions were prepared with boiled and argon-saturated double-deionized high-purity water ( $18.2\text{ M}\Omega\text{ cm}$ ) obtained from a Maxima (USF Elga) cartridge system designed for trace analysis. All solids were carefully weighed on a Precisa 262SMA-FR balance accurate to  $\pm 0.01$  mg. Ligand stock solutions were prepared by dissolving a weighed amount of compound in 1 mL of pure methanol in a 10 mL volumetric flask containing the appropriate amount of NaCl to reach a final concentration of 0.1 M. The flask was then filled up to the mark with an aqueous formate/formic acid buffer solution ( $\text{pH} = 3.71$ ,  $c = 25$  mM). The europium chloride mother solution (4.04 mM) was prepared likewise, although the quantity of added NaCl was adjusted to 0.088 M in order to keep the total chloride concentration constant at 0.1 M.

Titration were performed in a quartz cell (Hellma) of 1 cm optical path length containing 0.10 mL of the ligand stock

solution, 1.70 mL of aqueous buffer, and 0.20 mL of pure methanol ( $V_0 = 2.00$  mL) by manual addition of aliquots of the  $\text{EuCl}_3$  mother solution with the help of a Gilmont micropipette ( $2\ \mu\text{L}$  resolution). UV–Vis electronic absorption spectra were collected in the 250–500 nm range at a uniform data point interval of 1 nm with a Cary 50 (Varian) spectrophotometer equipped with a double-jacketed cell holder connected to a RE 106 (Lauda) water circulator ensuring a constant temperature of  $25.0 \pm 0.2^\circ\text{C}$ . Equilibration time between each incremental addition of the  $\text{EuCl}_3$  solution was found to be fast in all cases, as identical spectra were obtained by cycling the recordings with a 2 min delay between two consecutive measurements.

The entire multiwavelength data sets consisting of at least 13 spectra were decomposed in their principal components by factor analysis before refining the apparent equilibrium constants and extinction coefficients by a nonlinear least-squares procedure implemented in the Specfit program [36,37]. The goodness-of-fit was assessed by comparing the standard deviation of the fit ( $\sigma$ ) to the experimental noise level ( $< 0.003$ ), by visually inspecting the residuals, and by the physical meaning of the calculated electronic absorption spectra. All reported uncertainties correspond to the standard deviation of the refined parameters that were returned by the fitting software.

### 3. Theory

Complexation of europium(III) by phosphonate ligands (L) can be described by the following equilibrium:



where charges are omitted for sake of clarity. Since all equilibrium studies were carried out in buffered solutions, the actual protonation states of both the ligand and complex, along with the number of released protons can be ignored. The corresponding apparent overall formation constant  $\beta_{ij}$  is expressed by Eq. (4), where  $[\text{Eu}_i\text{L}_j]$ ,  $[\text{Eu}]$ , and  $[\text{L}]$  are the equilibrium concentrations of complex ( $[\text{Eu}_i\text{L}_j] = \sum [\text{Eu}_i(\text{LH}_k)_j]$ ), free metal, and uncomplexed ligand ( $[\text{L}] = \sum [\text{LH}_k]$ ), respectively.

$$\beta_{ij} = \frac{[\text{Eu}_i\text{L}_j]}{[\text{Eu}]^i[\text{L}]^j} \quad (4)$$

ACE allows direct monitoring of dynamic binding equilibria through analysis of the electrophoretic mobility shifts of L after addition of increasing amounts of metal cation in the separation buffer. Under such circumstances, the effective electrophoretic mobility,  $\mu_{ep}^L$ , can be expressed according to Eq. (5), where  $x_L$ ,  $\mu_{epL}$ ,  $x_{Eu_iL_j}$ , and  $\mu_{epEu_iL_j}$  are the molar fractions and the effective electrophoretic mobility of the free solute L and electrophoretic mobilities of the various  $Eu_iL_j$  species, respectively.

$$\mu_{ep}^L = x_L \mu_{epL} + \sum_{i=1}^n \sum_{j=1}^m x_{Eu_iL_j} \mu_{epEu_iL_j} \quad (5)$$

In the case where only a 1:1 metal–ligand complex is formed, Eq. (5) reduces to the following expression:

$$\mu_{ep}^L = \frac{\mu_{epL} + \mu_{epEuL} \beta_{11} [Eu]}{1 + \beta_{11} [Eu]} \quad (6)$$

For systems giving rise to two overlapping equilibria associated with the formation of both a mono- and a binuclear  $EuL$  and  $Eu_2L$  species, the observed electrophoretic mobility is given by Eq. (7), where  $K_{11}$  ( $K_{11} = \beta_{11}$ ) and  $K_{21}$  ( $K_{21} = \beta_{21}/\beta_{11}$ ) stand for the stepwise binding constants.

$$\begin{aligned} \mu_{ep}^L &= \frac{\mu_{epL} + \mu_{epEuL} \beta_{11} [Eu] + \mu_{epEu_2L} \beta_{21} [Eu]^2}{1 + \beta_{11} [Eu] + \beta_{21} [Eu]^2} \\ &= \frac{\mu_{epL} + \mu_{epEuL} K_{11} [Eu] + \mu_{epEu_2L} K_{11} K_{21} [Eu]^2}{1 + K_{11} [Eu] + K_{11} K_{21} [Eu]^2} \end{aligned} \quad (7)$$

Provided the total metal concentration is in large excess over that used for the ligand, the approximation  $[Eu] = [Eu]_{tot} - \sum_i [Eu_iL_j] \approx [Eu]_{tot}$  holds for the free europium concentration at equilibrium. As a consequence, the formation constants  $K_{ij}$  together with the intrinsic electrophoretic mobilities  $\mu_{epEu_iL_j}$  can be directly adjusted by nonlinear least-squares analysis of the  $(\mu_{ep}^L, [Eu]_{tot})$  data pairs.

In the simplest situation of a 1:1 binding event, three mathematical transformations of Eq. (6) afford linear plots which are generally referred to as the double reciprocal,  $y$ -reciprocal, and  $x$ -reciprocal. Although of common practice, computation of the three unknown parameters  $K_{11}$ ,  $\mu_{epL}$ , and  $\mu_{epEuL}$  by linear regression should be avoided as this procedure is well-known to return biased estimates. Nevertheless, Bowser and Chen have pointed out that a graphical representation of the experimental data according to Eq. (8), the so-called  $x$ -reciprocal form of Eq. (6), is a most valuable diagnostic tool for ascertaining the exclusive formation of a 1:1 complex provided a straight line is obtained [38].

$$\frac{\mu_{ep}^L - \mu_{epL}}{[Eu]} = -K_{11}(\mu_{ep}^L - \mu_{epL}) + K_{11}(\mu_{epEuL} - \mu_{epL}) \quad (8)$$

Departure from linearity was shown to be highly sensitive to the presence of additional higher-order metal complexes in equilibrium with the 1:1 binding stoichiometry. In the particular case of simultaneous formation of 1:1 and 1:2 (or 2:1) adducts, the concave or convex shape of the curve does not only enable to detect the occurrence of a dileptic (or dinuclear) complex, but also reflects the anti-cooperative ( $K_{11}/K_{12}$  or  $K_{11}/K_{21} > 4$ ) or cooperative ( $K_{11}/K_{12}$  or  $K_{11}/K_{21} < 4$ ) nature of the binding interaction. However, there is one limiting case where  $x$ -reciprocal plots remain linear and thus are unable to reveal the presence of the higher order 1:2 or 2:1 complexes, that is statistical binding ( $K_{11}/K_{12}$  or  $K_{11}/K_{21} = 4$ ) with microscopic species sharing identical mobilities [39]. In practice, such a situation is extremely rare, but when the values of the equilibrium constants are close to the statistical factors, the slight curvature in the plot might be obscured by random error associated with the data.

## 4. Results and discussion

The potentialities offered by a hyphenated electromigration technique for the rapid screening of the europium(III) binding affinity of 15 different P=O containing molecules have been evaluated by taking advantage of the sensitive detection of the naturally occurring  $^{31}P$  isotope by ICP-MS. For some relevant systems, quantitative speciation results derived by this methodology have also been confronted to UV-Vis spectrophotometric titration data for validation purposes. Although several ligands considered herein (8–15) possess acidic binding groups (e.g. phosphonic acid, aminocarboxylic acid, and phenol), no attempts were made to define their exact protonation state at the working pH value of 3.7. Hence, the tested organic compounds will be designated hereafter by L, although it should be kept in mind that each of these chelators might exist as a mixture of several partially protonated species, while the aminodi-carboxylic acids 13–15 behave as zwitterions. For compounds 8–12, 14, and 15, the phosphonic acid groups are expected to predominate in their negatively charged  $-PO_3H^-$  form at pH 3.7 since their first  $pK_a$  in aqueous solutions is typically around 2 or slightly below, while the second deprotonation occurs around neutrality [40,41]. In the case of the methyl ester derivative 13, almost total deprotonation of the P–OH functionality is also expected at pH 3.7 considering the  $pK_a$  values of about 1.5 reported for the  $-PO(OH)(OR)$  moieties [40,41].

### 4.1. Affinity screening of the phosphorus-containing ligands for europium(III)

For rapid screening analysis, the fused-silica capillary was coated with the cationic polymer polybrene. As a consequence, the ionization extent of the inner surface is not pH-dependent, leading to a high electroosmotic flow, close to  $-3.5 \times 10^{-8} \text{ m}^2 \text{ V}^{-1} \text{ s}^{-1}$  (five times more important than without polybrene) even for slightly acidic solutions (pH=3.7). In a first step, ca. 0.1 mM ligand solutions were analyzed in order to select the most powerful europium(III) chelators. For each of the fifteen compounds selected in this work (Fig. 1), effective  $\mu_{ep}^L$  values were successively determined using two electrolytes: one containing 30 mM sodium chloride and the other one containing 10 mM  $EuCl_3$ . Experimental results are graphically displayed in Fig. 2. Moreover, it should be stressed that this screening strategy requires no more than 5 ng of compound and takes approximately one hour per ligand, including the capillary washing time and conditioning steps.

Examination of the results displayed in Fig. 2 leads to the following conclusions: neither the diphosphine oxides 1–6 nor the mixed phosphine oxide-thiophosphine 7 exhibited any appreciable affinity towards europium(III) taken in 100-fold excess in the water-rich medium. This lack of affinity is a direct consequence of both the high hydration energy of this trivalent  $Eu^{3+}$  cation and the weak electron donating ability of P=O and P=S groups. In turn, phosphonic acids 8–15 possess between 2 and 5 ionizable groups with typical  $pK_a$  values spanning a wide range of at least 6 orders of magnitude. Accordingly, their metal affinity is expected to be strongly pH dependent in contrast to that of the neutral phosphine oxide derivatives 1–7. Hence, a significant change in effective  $\mu_{ep}^L$  values was observed at pH 3.7 for compounds 8–15 in the presence of europium salt, indicating formation of complexes. Moreover, the effective mobilities were significantly higher than those found for the ligands alone, while they became even positive in some cases (8, 9, 11, 12, 14, 15). This is in agreement with a reduction of the overall electrical charge of the ligand upon metal uptake. Accordingly, the most powerful  $Eu^{3+}$  binders appear to be 9, 14, and 15.



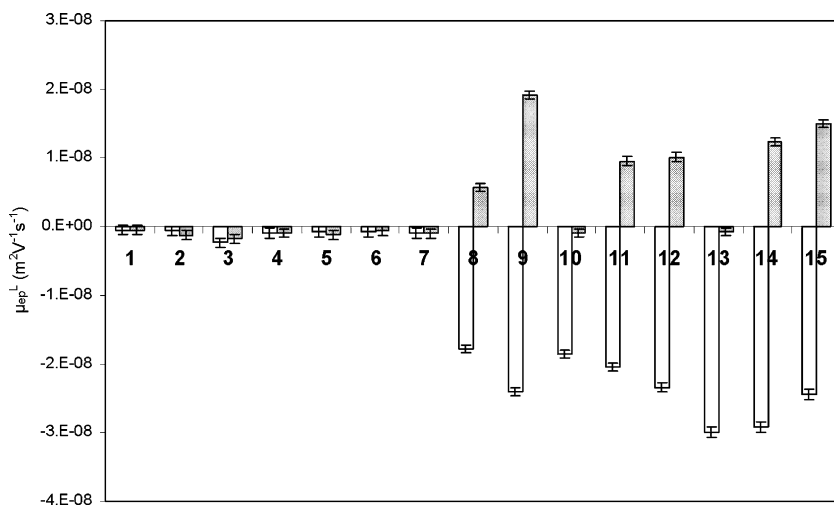


**Fig. 2.** Effective electrophoretic mobility monitored by ICP-MS at  $m/z = 31$  of the phosphorylated compounds in the absence or presence of  $\text{Eu}^{3+}$  in the electrolyte. Electrolyte: 25 mM aqueous formic acid/formate buffer at pH 3.7 containing 10% (v/v) methanol and either 30 mM NaCl (white bars) or 10 mM  $\text{EuCl}_3$  (grey bars); capillary: fused silica, 70 cm  $\times$  75  $\mu\text{m}$  i.d. modified by dynamic coating with 0.1% (m/m) polybren (under its chloride form); injection pressure: 3.45 kPa; injection time: 5 s; migration conditions:  $-20$  kV;  $T = 298$  K.

#### 4.2. Determination of the apparent association constants by CE-ICP-MS

Prompted by the encouraging screening experiments, compounds **8–15** were subjected to further investigations in order to determine the apparent association constants by capillary electrophoresis. For that purpose, the migration time was monitored as a function of the total  $\text{EuCl}_3$  concentration introduced in the electrolyte, which was always in large excess with respect to the ligand. For each system, about ten runs were carried out. As an example, Fig. 3 reproduces a selection of the electropherograms recorded for compound **11** and increasing europium(III) concentrations.

As a general feature, a single peak was observed whatever the lanthanide content, indicating fast metal/ligand exchange kinetics and suggesting the formation of labile complexes. Graphical data preprocessing according to Eq. (8) was systematically performed in order to detect higher binding stoichiometries than the 1:1 species in the presence of a large excess of metal over ligand. Indeed, these experimental conditions might favor in some instances the formation of polynuclear, most probably dinuclear, complexes in addition to the  $\text{EuL}$  form. Fig. 4 displays the  $x$ -reciprocal form of the binding isotherm for each considered binder. Linear plots have been obtained for the three monophosphonic compounds **8**, **10**, and **11**, strongly supporting the presence of a single complex of 1:1 stoichiometry at equilibrium. In contrast, the  $x$ -reciprocal plots

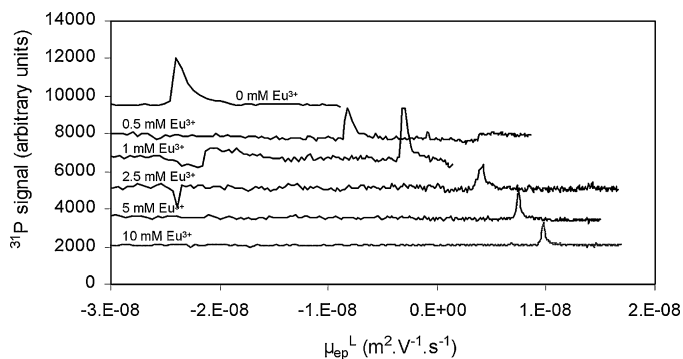


**Fig. 3.** Variation of the effective electrophoretic mobility of compound **11** as a function of the total  $\text{EuCl}_3$  concentration introduced in the electrolyte. Experimental conditions are identical to those given in Fig. 2.

pertaining to the diphosphonic acids **9**, **12**, and **15**, but also to the methylphosphonate iminodiacetic acid derivative **14**, show a nonlinear behavior when a 1:1 binding model was assumed. As pointed out in Section 3.1, curvature rules out the sole formation of the  $\text{EuL}$  species and highlights the occurrence at equilibrium of at least one more stable polynuclear complex. Under the dilute conditions employed herein, cluster-type structures are most unlikely. However, dinuclear  $\text{Eu}_2\text{L}$  compounds might be expected to form considering both the large excess of metal in the supporting electrolyte and the potential ditopic nature of ligands **9**, **12**, **14**, and **15**, which incorporate two strongly coordinating functions (either two phosphonates or one phosphonate and one iminodiacetate).

Based on the above rationale, the binding isotherms were all adjusted by nonlinear least-squares analysis using either Eq. (6) or (7) when the speciation model comprised both the  $\text{EuL}$  and  $\text{Eu}_2\text{L}$  complexes. The complexation constants together with the calculated mobilities obtained at convergence by minimizing the  $\sigma^2$  error function are summarized in Table 2, while Fig. 5 shows as illustrative examples both the experimental and the theoretical binding isotherms obtained for compounds **11** and **9**. Overall, excellent fits were obtained for **8**, **10**, and **11** by assuming the sole formation of a 1:1 complex as suggested by the linear  $x$ -reciprocal

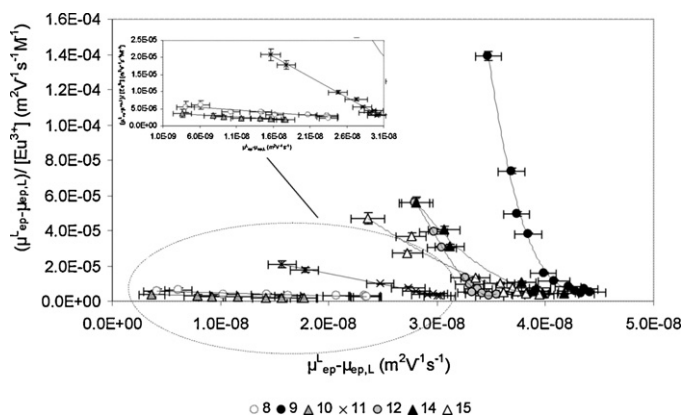


**Fig. 4.**  $x$ -reciprocal plots assuming a 1:1 complex formation model of the binding isotherms. Straight lines obtained by linear regression support the exclusive formation of  $\text{EuL}$  species. The curved lines were drawn as an eye guide and evidence the occurrence of additional dinuclear complexes. Experimental conditions are identical to those given in Fig. 2.

**Table 2**  
Refined thermodynamic parameters and electrophoretic mobilities of europium complexes.<sup>a</sup>

Ligand	$\log K_{11}$	$\log K_{21}$	$\mu_{epL} \times 10^8 \text{ (m}^2 \text{ V}^{-1} \text{ s}^{-1}\text{)}$	$\mu_{epML} \times 10^8 \text{ (m}^2 \text{ V}^{-1} \text{ s}^{-1}\text{)}$	$\mu_{epM2L} \times 10^8 \text{ (m}^2 \text{ V}^{-1} \text{ s}^{-1}\text{)}$
<b>8</b>	$2.1 \pm 0.1$	b	$-1.69 \pm 0.08$	$2.4 \pm 0.6$	b
<b>9</b>	$4.6 \pm 0.2$	$2.2 \pm 0.3$	$-2.41 \pm 0.05$	$1.3 \pm 0.1$	$2.4 \pm 0.3$
<b>10</b>	$2.0 \pm 0.1$	b	$-1.78 \pm 0.04$	$1.8 \pm 0.5$	b
<b>11</b>	$3.2 \pm 0.1$	b	$-2.1 \pm 0.2$	$1.1 \pm 0.1$	b
<b>12</b>	$3.87 \pm 0.05$	c	$-2.34 \pm 0.06$	$1.01 \pm 0.03$	c
<b>14</b>	$3.60 \pm 0.05$	d	$-2.9 \pm 0.1$	$1.15 \pm 0.06$	d
<b>15</b>	$3.44 \pm 0.05$	d	$-2.4 \pm 0.1$	$1.49 \pm 0.06$	d

<sup>a</sup> Solvent: 25 mM aqueous formic acid/formate buffer at pH 3.7 containing 10% (v/v) methanol;  $[\text{Cl}^-]_{\text{tot}} = 30 \text{ mM}$ ;  $T = 298 \text{ K}$ . Reported errors correspond to the standard deviation.

<sup>b</sup> Not detected.

<sup>c</sup> Refinement of the parameter according to Eq. (5) was unsuccessful due to divergence of the minimization procedure, although formation of the  $\text{Eu}_2\text{L}$  species cannot be excluded considering the curved  $x$ -reciprocal plot.

<sup>d</sup> Data processing according to Eq. (5) returned at convergence an unrealistic value, although formation of the  $\text{Eu}_2\text{L}$  species cannot be excluded considering the curved  $x$ -reciprocal plot.

plots. While the binding isotherm for **11** shows a plateau at higher europium concentrations (Fig. 5a), the lower affinity of **8** and **10** for  $\text{Eu}^{3+}$  prevented to reach a constant end-value. The mathematical treatment of experimental data according to Eq. (6) returns usually highly correlated estimates of both  $K_{11}$  and  $\mu_{epEuL}$ , which is an intrinsic difficulty because of the optimization of the product  $K_{11}\mu_{epEuL}$  appearing in the numerator. As a matter of facts, independent estimation of  $K_{11}$  requires a large number of data points in the europium concentration range where  $\text{EuL}$  is the predominant species. Since this situation could not be achieved for **8** and **10**, the effective uncertainties associated to both parameters  $K_{11}$  and  $\mu_{epEuL}$  are probably larger than the standard deviations derived from the variance/covariance matrix [23].

In agreement with the curved  $x$ -reciprocal plot found for the diposphonic acid **9**, the goodness of fit of the corresponding binding isotherm was clearly improved by considering the stepwise formation of both  $\text{EuL}$  and  $\text{Eu}_2\text{L}$  complexes instead of a single species. The inappropriateness of Eq. (6) to properly model the

experimental readings might be difficult to recognize from Fig. 5b, but it becomes clearly apparent if the europium concentrations are plotted on a logarithmic scale as shown in the inset of Fig. 5b. For the same reasons as those outlined above, the errors on both equilibrium constants are rather large with a relative standard deviation on  $\log K_{21}$  exceeding 13% in spite of the low scattering of the points. The distribution diagram of free and metal-bound ligand species corresponding to the analytical conditions ( $[\text{L}]_{\text{tot}} = 0.1 \text{ mM}$ ) indicates that the fraction of  $\text{EuL}$  reaches its maximum at 89% for a total europium concentration of 0.5 mM (5-fold excess), while the proportion of free L and  $\text{Eu}_2\text{L}$  is approximately equal to 5% each. At the highest metal concentration used in this work ( $[\text{Eu}]_{\text{tot}} = 10 \text{ mM}$ ), both  $\text{EuL}$  and  $\text{Eu}_2\text{L}$  are in equilibrium in a 39:61 molar ratio. Accordingly, all three species contribute significantly to the overall effective mobility  $\mu_{ep}^L$ , providing some additional confidence to the refined stability constants.

A more intricate situation was encountered with compounds **12**, **14**, and **15**. On the one hand, the nonlinear  $x$ -reciprocal plots displayed in Fig. 4 suggest the occurrence of at least one additional species in equilibrium with the  $\text{EuL}$  complex. On the other hand, all attempts to refine the five unknown parameters of Eq. (7) failed due to divergence in the case of ligand **12**, while for the two other binders, the nonlinear least-squares procedure returned unrealistic estimates for  $K_{21}$  and/or  $\mu_{epEu_2L}$ , with relative standard deviations exceeding 100% at convergence. Due to the unavoidable correlation between the refined equilibrium constant and the associated intrinsic mobility, it becomes obviously even more difficult when these contribute only marginally to the measured signal. The low information content of the raw data with respect to the additional species might explain why extraction of  $K_{21}$  and  $\mu_{epEu_2L}$  becomes impossible, although a low abundance of a few percents of  $\text{Eu}_2\text{L}$  might be sufficient for observing departures from linearity in  $x$ -reciprocal plots. Hence, the binding isotherms for these three ligands were satisfactorily adjusted to a single equilibrium model by using Eq. (6), as proven by the almost identical residual standard deviation obtained for fits performed with Eq. (7). Nevertheless, the calculated  $K_{11}$  values reported in Table 2 for **12**, **14**, and **15** should be considered as less reliable than those found for the four other compounds.

Interestingly, the intrinsic mobilities  $\mu_{epL}$  estimated for the seven chelators are consistent with their prevalence at pH 3.7 as partially deprotonated anions bearing a similar charge close to  $-1$ , as can be inferred from structural considerations. Their magnitude ranges between  $-2.9$  and  $-1.7 \times 10^{-8} \text{ m}^2 \text{ V}^{-1} \text{ s}^{-1}$ , while individual values tend to be higher for diposphonic or mixed phosphonic–aminocarboxylic acids. Complex formation leads to a systematic decrease of the mobility as all refined  $\mu_{epEuL}$  and  $\mu_{epEu_2L}$  values are positive and comprised between 1 and

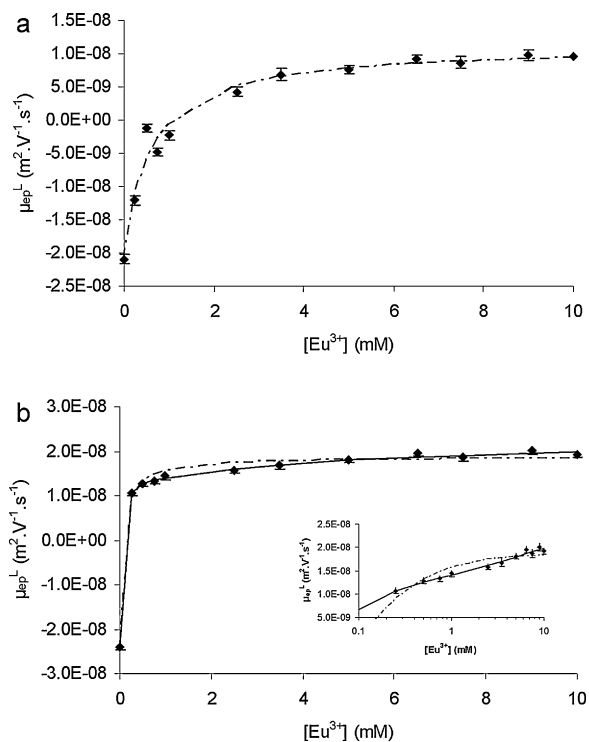


**Fig. 5.** Binding isotherm for compounds **11** (a) and **9** (b) assuming formation of either a single species of 1:1 stoichiometry (dashed line) or of both  $\text{EuL}$  and  $\text{Eu}_2\text{L}$  complexes (full line). Experimental conditions are identical to those given in Fig. 2.

$2.4 \times 10^{-8} \text{ m}^2 \text{ V}^{-1} \text{ s}^{-1}$ . These figures are also fully consistent with the formation of cationic europium(III) species as might be anticipated if the chelators are prevailing in their  $\text{LH}_k^-$  forms.

#### 4.3. Spectrophotometric validation studies

In order to validate the apparent binding constants measured on the nanogram scale by CE-ICP-MS, the affinity of some ligands towards europium was also investigated by a standard titration technique. Since organic material prepared according to combinatorial synthetic approaches is usually available in low amounts (*i.e.* few milligrams), a sensitive alternative analytical technique was required. For compounds **1–12**, UV-Vis absorption spectrophotometry appeared as the method of choice compared to classical glass-electrode potentiometry, because the aromatic substituents borne by the phosphorus atoms act as efficient absorbing units and thus enabled to probe metal-binding through the electronic perturbations experienced by these chromophores. Therefore, europium titrations were monitored spectrophotometrically between 250 and 500 nm in the buffered water/methanol 90:10 (v/v) mixture by maintaining both the pH and the total chloride concentration constant at 3.7 and 0.1 M, respectively, in order to reproduce as closely as possible the experimental conditions used during the electrophoretic measurements.

According to UV-Vis spectroscopy, none of the investigated diphosphine oxide exhibits any measurable affinity towards  $\text{Eu}^{3+}$  in the water-rich binary solvent used throughout. This behavior has been unambiguously confirmed in the case of chelator **1**, since any significant spectral changes could be detected upon addition of up to 100 equiv. of the lanthanide salt in water/methanol 90:10 (v/v). For compounds **2–7**, the lack of affinity can moreover be explained by structural features as it is well-known that chelate rings comprising more than six atoms are unstable [42]. However, decreasing the solvent polarity by increasing the methanol content favored the europium uptake by the neutral ligand **1**. Numerical processing with the Specfit program of the titration data collected in the non-buffered binary water/methanol 10:90 (v/v) mixture (addition of acid induced no spectral change) evidenced the exclusive formation of a single complex of 1:1 stoichiometry, albeit of moderate stability ( $\log K_{11} = 3.6 \pm 0.2$ ,  $I = 0.1 \text{ M N}(n\text{-C}_4\text{H}_9)_4\text{Cl}$ ,  $T = 25.0(2)^\circ\text{C}$ ). The calculated absorption data for each limiting species reflect the hyperchromic effect undergone by the phenyl centered  $\pi\text{-}\pi^*$  transitions of ligand **1** ( $\lambda_{\text{max}} = 260.5 \text{ nm}$ ,  $\epsilon = 1990 \text{ M}^{-1} \text{ cm}^{-1}$ ;  $\lambda_{\text{max}} = 266.5 \text{ nm}$ ,  $\epsilon = 2640 \text{ M}^{-1} \text{ cm}^{-1}$ ; and  $\lambda_{\text{max}} = 273.4 \text{ nm}$ ,  $\epsilon = 2160 \text{ M}^{-1} \text{ cm}^{-1}$  – these data are in excellent agreement with the experimentally measured values), upon formation of the  $[\text{Eu}(\mathbf{1})]^{3+}$  species ( $\lambda_{\text{max}} = 261.1 \text{ nm}$ ,  $\epsilon = 2290 \text{ M}^{-1} \text{ cm}^{-1}$ ;  $\lambda_{\text{max}} = 266.8 \text{ nm}$ ,  $\epsilon = 3280 \text{ M}^{-1} \text{ cm}^{-1}$ ; and  $\lambda_{\text{max}} = 273.4 \text{ nm}$ ,  $\epsilon = 2720 \text{ M}^{-1} \text{ cm}^{-1}$ ). Simultaneous binding of both P=O groups that leads to a six-membered chelate cycle is fully supported by the structure of the double-complex salt  $[\text{Eu}(\mathbf{1})_2(\text{NO}_3)_2][\text{Eu}(\mathbf{1})(\text{NO}_3)_4]$  that crystallized out of  $\text{CH}_3\text{CN}$  solutions for  $[\text{Eu}]/[\mathbf{1}]$  concentration ratios comprised between 0.67 and 1 [43]. Since formation of polyleptic europium complexes with ligand **1** are favored in weakly dissociating media in the presence of an excess of ligand [43,44], it is not surprising that these species could not be detected by UV-Vis spectrophotometry under the chosen experimental conditions.

Relying on the quantitative affinity scale established by CE-ICP-MS (Table 2), 2-hydroxy-3-phosphono-benzoic acid **11** is a chelator of moderate strength, because most of the potential binding groups remain, at least partially, protonated at pH 3.7. It appeared therefore as the ideal system for validation purposes. Considering a molar extinction coefficient value of  $2590 \text{ M}^{-1} \text{ cm}^{-1}$  at the absorption band maximum ( $\lambda_{\text{max}} = 315 \text{ nm}$ ), a concentration of *ca.* 0.35 mM

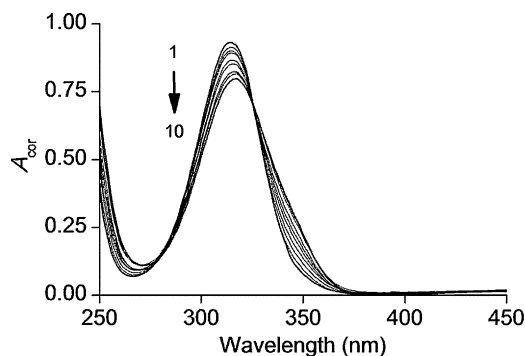


**Fig. 6.** Spectrophotometric titration of compound **11** as a function of increasing amounts of  $\text{EuCl}_3$ . Solvent: 25 mM aqueous formic acid/formate buffer at pH 3.7 containing 10% (v/v) methanol;  $I = 0.1 \text{ M NaCl}$ ;  $T = 298.2(2) \text{ K}$ ;  $[\mathbf{11}]_{\text{tot}} = 0.35 \text{ mM}$ ;  $[\text{EuCl}_3]_{\text{tot}} = 4.04 \text{ mM}$ ;  $V_0 = 2 \text{ mL}$ ;  $l = 1 \text{ cm}$ . Dilution-corrected spectra 1–10: 0.29, 0.58, 0.87, 1.16, 1.74, 2.32, 3.48, 4.64, 6.38, 8.7 equiv. of  $\text{Eu}^{3+}$ .

enabled to perform thermodynamic measurements with  $150 \mu\text{g}$  of substance per experiment. Metal binding was clearly ascertained by the progressive broadening, hypochromic and slight bathochromic shifts undergone by the featureless absorption band of **11** upon incremental addition of  $\text{EuCl}_3$  (Fig. 6). Moreover, the occurrence of an isosbestic point at 325 nm suggests a single equilibrium. Singular value decomposition of the entire data set further supported the presence of only two absorbing components, including unbound ligand and one europium complex. Subsequent data refinement using more than one complexed species failed due to systematic divergence of at least one adjusted parameter. Statistical analysis further established the 1:1 metal-ligand stoichiometry ( $\lambda_{\text{max}} = 320 \text{ nm}$ ,  $\epsilon = 2000 \text{ M}^{-1} \text{ cm}^{-1}$ ) that could be deduced from the electromigration studies carried out using *ca.*  $10^5$ -fold smaller volumes. The value of the apparent binding constant returned by Specfit after spectral deconvolution ( $\log K_{11} = 3.1 \pm 0.2$ ) was in excellent agreement with the one obtained by CE-ICP-MS ( $\log K_{11} = 3.2 \pm 0.1$ ) under similar working conditions (Table 2). This agreement definitively validates the experimental procedure developed for exploring the metal-ion speciation both from a qualitative (*i.e.* number and stoichiometry of major species) and quantitative (*i.e.* accurate determination of apparent binding constants) point of view.

## 5. Conclusion

The performances of hyphenated capillary electrophoresis for screening a library of chelators with respect to their relative metal-binding affinity in buffered hydromethanolic solutions have been evaluated by taking advantage of the high sensitivity and selectivity of ICP-MS for detecting phosphorous at the ppt level. Monitoring the signal of a ligand-incorporated heteroatom instead of the metal ion, as it is common practice in affinity capillary zone electrophoresis, has been shown to be highly advantageous when the organic chelating agents are available only in minute quantities. Detection limits of elemental phosphorous ranged between 2 and  $25 \mu\text{mol L}^{-1}$ , depending on the phenomena contributing to the peak widening for each ligand. Our methodology is therefore particularly well-adapted for screening libraries of chemicals obtained by combinatorial synthesis.

As a proof of principle, a set of fifteen phosphorylated products ranging from neutral aprotic diphosphine oxides to polyfunctional mono- and diphosphonic acids has been selected. Regardless of their acid-base properties and structures, a relative affinity scale towards europium(III) could be established at constant pH by simple comparison of the electrophoretic mobility of each ligand measured first in the absence and then in the presence of the

targeted metal cation. Since the latter is introduced in the electrolyte in large excess, the fast selection of the most affine organophosphorus derivatives could be achieved by consuming no more than 5 ng of each substance. Most importantly, this analytical procedure could also be applied for quantitative speciation studies at the trace level (5–20 ng), where the classical potentiometric and spectroscopic techniques lack sensitivity. Numerical processing of the average ligand mobility variations induced by increasing amounts of europium salt in the electrolyte returned reliable values of conditional binding constants, even in the case of two overlapping equilibria associated to the concomitant formation of two moderately weak  $\text{EuL}$  and  $\text{Eu}_2\text{L}$  complexes at a fixed pH. The accuracy of the thereby determined equilibrium constants ranging between  $10^2$  and  $\sim 5 \times 10^4 \text{ M}^{-1}$ , as well as the reliability of the derived chemical model, was ascertained by conducting spectrophotometric titrations which required  $10^5$ -fold higher sample volumes. It turns out that CE-ICP-MS as implemented in this work appears as a powerful mean to investigate the speciation of systems involving complex equilibria under high-dilution, which is especially well-adapted when ligand and/or metal salts are precious due to their low availability. Hence, it should be a promising method for solution thermodynamic investigations of actinides or toxic metal ions in environmentally-relevant conditions. Furthermore, the use of a ICP-MS detector also opens new perspectives as it could be easily extended to other classes of ligands incorporating heteroatoms other than phosphorus, like sulfur (e.g. cysteine-based polypeptides), or halogens (mainly iodine).

## Acknowledgements

This work was supported by the Agence Nationale pour la Recherche (ANR project “Chelan” No. 06-BLAN-0198), the Centre National de la Recherche Scientifique (CNRS), the Ministère de la Recherche et de l'Enseignement Supérieur, and the Conseil Régional de Bourgogne. The authors would like to thank J.-F. Dufrêche (Institut de Chimie Séparative de Marcoule, France) for fruitful discussions.

## References

- [1] O. Lavastre, F. Bonnet, L. Gallard, *Curr. Opin. Chem. Biol.* 8 (2004) 311.
- [2] J. Kyranos, J. Hogan, *Anal. Chem.* 70 (1998) 389A.
- [3] A.E.V. Gorden, J. Xu, K.N. Raymond, P. Durbin, *Chem. Rev.* 103 (2003) 4207.
- [4] H.H. Dam, H. Beijleveld, D.N. Reinhoudt, W. Verboom, *J. Am. Chem. Soc.* 130 (2008) 5542.
- [5] H.H. Dam, D.N. Reinhoudt, W. Verboom, *Chem. Soc. Rev.* 36 (2007) 367.
- [6] M. Sawicki, J.-M. Siaugue, C. Jacopin, C. Moulin, T. Bailly, R. Burgada, S. Meunier, P. Baret, J.-L. Pierre, F. Taran, *Chem. Eur. J.* 11 (2005) 3689.
- [7] Y. Lin, D. Bernardi, E. Doris, F. Taran, *Synlett* (2009) 1466.
- [8] V. Moulin, C. Moulin, *Radiochim. Acta* 89 (2001) 773.
- [9] G. Plancque, V. Moulin, P. Toulhoat, C. Moulin, *Anal. Chim. Acta* 478 (2002) 11.
- [10] C. Moulin, *Radiochim. Acta* 91 (2003) 651.
- [11] T. Vercouter, P. Vitorge, B. Amekraz, E. Giffaut, S. Hubert, C. Moulin, *Inorg. Chem.* 44 (2005) 5833.
- [12] H. Moll, M. Glorius, G. Bernhard, *Bull. Chem. Soc. Jpn.* 81 (2008) 857.
- [13] S. Colette, B. Amekraz, C. Madic, L. Berthon, G. Cote, C. Moulin, *Inorg. Chem.* 43 (2004) 6745.
- [14] T. Vercouter, P. Vitorge, N. Trigoulet, E. Giffaut, C. Moulin, *New J. Chem.* 29 (2005) 544.
- [15] A. Heller, O. Rönitz, A. Barkleit, G. Bernhard, J.-U. Ackermann, *Appl. Spectrosc.* 64 (2010) 930.
- [16] C. Jiang, D.W. Armstrong, *Electrophoresis* 31 (2010) 17.
- [17] X. Liu, F. Dahdouh, M. Salgado, F.A. Gomez, *J. Pharm. Sci.* 98 (2009) 394.
- [18] Z. Chen, S.G. Weber, *Trends Anal. Chem.* 27 (2008) 738.
- [19] S. Ehala, J. Mišek, I.G. Stará, I. Starý, V. Kašička, *J. Sep. Sci.* 31 (2008) 2686.
- [20] R. Plasson, H. Cottet, *Anal. Chem.* 78 (2006) 5394.
- [21] S. Ehala, E. Makrlík, P. Toman, V. Kašička, *Electrophoresis* 31 (2010) 702.
- [22] J. Petit, V. Geertsen, C. Beaucaire, M. Stambouli, *J. Chromatogr. A* 1216 (2009) 4113.
- [23] J. Petit, J. Aupiais, S. Topin, V. Geertsen, C. Beaucaire, M. Stambouli, *Electrophoresis* 31 (2010) 355.
- [24] S. Topin, J. Aupiais, N. Baglan, T. Vercouter, P. Vitorge, P. Moisy, *Anal. Chem.* 81 (2009) 5354.
- [25] M. Girardot, P. Gareil, A. Varenne, *Electrophoresis* 31 (2010) 546.
- [26] S. Ehala, V. Kašička, E. Makrlík, *Electrophoresis* 29 (2008) 652.
- [27] S. Ehala, J. Dybal, E. Makrlík, V. Kašička, *J. Chromatogr. A* 1216 (2009) 3660.
- [28] S. Safi, Z. Asfari, M. Leroy, C. Basset, E. Quéméneur, C. Vidaud, A. Hagège, *Analyst* 134 (2009) 256.
- [29] Y.-H. Chu, Y.M. Dunayevskiy, D.P. Kirby, P. Vouros, B.L. Karger, *J. Am. Chem. Soc.* 118 (1996) 7827.
- [30] L. Yi, L. Xiaomei, F. Hui, Z. Yingcheng, L. Dan, W. Ying, *J. Chromatogr. A* 1143 (2007) 284.
- [31] T. Le Saux, A. Varenne, F. Perreau, L. Siret, S. Duteil, L. Duhau, P. Gareil, *J. Chromatogr. A* 1132 (2006) 289.
- [32] J. Chamoun, A. Hagège, *J. Anal. At. Spectrom.* 20 (2005) 1030.
- [33] J. Chamoun, A. Hagège, *Radiochim. Acta* 93 (2005) 659.
- [34] M. Dell'Mour, G. Koellensperger, J.P. Quirino, P.R. Haddad, C. Stanetty, E. Oburger, M. Puschenreiter, S. Hann, *Electrophoresis* 31 (2010) 1201.
- [35] Origin 6.0, Microcal Software Inc., Northampton, MA.
- [36] H. Gampp, M. Maeder, C.J. Meyer, A.D. Zuberbühler, *Talanta* 32 (1985) 95.
- [37] H. Gampp, M. Maeder, C.J. Meyer, A.D. Zuberbühler, *Talanta* 32 (1985) 257.
- [38] M.T. Bowser, D.D.Y. Chen, *Anal. Chem.* 70 (1998) 3261.
- [39] D.A. Deranleau, *J. Am. Chem. Soc.* 91 (1969) 4050.
- [40] A.E. Martell, R.M., Smith, R.J. Motekaitis, NIST Critically Selected Stability Constants of Metal Complexes Database, ver. 8.0, NIST Standard Reference Database No. 46, Gaithersburg, MD, 2004.
- [41] L.D. Pettit, K.J. Powell, The IUPAC Stability Constants Database, ver. 5.84, Academic Software and IUPAC, Otley, 2010.
- [42] A.E. Martell, R.D. Hancock, *Metal Complexes in Aqueous Solutions*, Plenum Press, New York, 1996.
- [43] A.M.J. Lees, A.W.G. Platt, *Inorg. Chem.* 42 (2003) 4673.
- [44] L. Huang, B.-Q. Ma, C.-H. Huang, T.C.W. Mak, G.-Q. Yao, G.-X. Xu, *J. Coord. Chem.* 54 (2001) 95.